ELSEVIER

Materials Characterization 58 (2007) 864–873

MATERIALS CHARACTERIZATION

Support effects on hydrotreating activity of NiMo catalysts

M.A. Domínguez-Crespo [a,b,*], E.M. Arce-Estrada [c], A.M. Torres-Huerta [d], L. Díaz-García [a], M.T. Cortez de la Paz [a]

[a] *Instituto Mexicano del Petróleo, Programa de Tratamiento de Crudo Maya. Avenida Eje Central Lázaro Cárdenas No.152, Col. San Bartolo Atepehuacan, 07730, México D. F. Mexico*

[b] *Instituto Politécnico Nacional, Grupo de Ingeniería en Procesamiento de Materiales CICATA-IPN, Unidad Altamira. Km 14.5, Carretera Tampico-Puerto Industrial Altamira, C. P. 89600, Altamira, Tamps. Mexico*

[c] *Instituto Politécnico Nacional, Departamento de Metalurgia y Materiales. A. P. 75-876, 07300 México, D. F. Mexico*

[d] *Universidad Nacional Autónoma de México, Instituto de Investigación en Materiales, Circuito Exterior s/n, Ciudad Universitaria. A.P. 70-360. Del. Coyoacán, C. P. 04510 México D. F. Mexico*

Received 9 January 2006; received in revised form 9 August 2006; accepted 23 August 2006

Abstract

The effect of the gamma alumina particle size on the catalytic activity of $NiMoS_x$ catalysts prepared by precipitation method of aluminum acetate at pH = 10 was studied. The structural characterization of the supports was measured by using XRD, pyridine FTIR–TPD and nitrogen physisorption. NiMo catalysts were characterized during the preparation steps (annealing and sulfidation) using transmission electron microscopy (TEM). Hydrogen TPR studies of the NiMo catalysts were also carried out in order to correlate their hydrogenating properties and their catalytic functionality. Catalytic tests were carried out in a pilot plant at 613, 633 and 653 K temperatures. The results showed that the rate constants of hydrodesulfurization (HDS), hydrodenitrogenation (HDN) and hydrodearomatizing (HDA) at 613–653 K decreased in the following order: A > B > C corresponding to the increase of NiMoS particle size associated to these catalysts.

Keywords: NiMoS particles; γ-Alumina crystal size; HDS

1. Introduction

The oil production of low-sulfur diesel fuels is currently an important topic in oil refineries due to more stringent environmental legislation [1,2]. Hydrodesulfurization (HDS) of refinery streams is carried out with catalysts consisting of Mo or W promoted with Co or Ni, all in the sulfide state [3]. In the preparation, sulfidation of the oxide precursors in a mixture of H_2S/H_2 or in the sulfur-containing hydrocarbon feed is an essential step. These sulfur compounds have shown interesting properties such as their ability to catalyze in the presence of hydrogen the removal of sulfur from heterocyclic organic molecules such as thiophene, benzothiophene and dibenzothiophene [4,6]. Some interesting researches have been developed to explain metal–support interaction. Topsoe et al. [1,5] have mentioned that the catalytic activity depends on the form, orientation and growth of MoS_2 species on the surface support. In addition, Prins et al. [7] have found that the MoS_2 has a layered lattice and that the sulfur–

* Corresponding author.
E-mail address: adcrespo2000@yahoo.com.mx (M.A. Domínguez-Crespo).

1044-5803/$ - see front matter © 2006 Elsevier Inc. All rights reserved.
doi:10.1016/j.matchar.2006.08.013

sulfur interactions between sandwich domains of MoS_2 layers on the surface support are weak. Other authors [8,9] have found that the MoS_2 clusters are controlled by the surface orientation and crystalline phase of the alumina. Sakashita et al. [9] have also observed an improvement of the HDT activity over NiCoMoS because of the presence of MoS_2 clusters on the edge planes [10,11]. As it can be observed, up to now, no clear information exist on the effect of the support particle size on the growth of MoS_2 species. Thus, the aim of this work is to study the effect of particle size on gamma alumina supports during NiMo catalyst preparation and its influence on the formation of metal-sulfided species. The performance of hydrotreating catalysts during hydrogenation of aromatics (HDA), hydrodesulfurization (HDS) and hydrodenitrogenation (HDN), using a heavy gas oil (HGO) as a real feedstock from Mexican crude, was also studied.

2. Experimental

2.1. Preparation of supports and catalysts

The synthesis of the γ-Al_2O_3 supports was carried out using the precipitation method of aluminum acetate in a vessel containing ammonia hydroxide at pH = 10. The material was heated at three different temperatures (293, 333 and 363 K) with 2, 4 and 18 h of nucleation time. The temperature and the nucleation time were controlled to obtain different particle sizes close to 3 (A), 5 (B) and 10 nm (C). During catalysts preparation, the molybdenum and nickel contents were adjusted to reach 11.5 wt.% and 2.9 wt.% nominal contents. The active component MoO_3 and the promoter NiO were supported using an ammonia solution through spray impregnation method [7,12]. The impregnated samples were dried with forced convection oven at 383 K (2 h) and then calcined in a furnace, using a heating rate of 5 K min^{-1} to 773 K (4 h).

2.2. Characterization

The textural properties of supports and catalysts were carried out in an ASAP 2000 Micrometrics instrument by means of nitrogen adsorption and desorption at 78 K with the BET and BJH methods.

Hydrogen TPR experiments were measured using an *in situ* Research Instrument (IRI) model RIG-100, provided with a flow reactor and a reducing mixture of hydrogen/argon (12 vol.% of H_2) and a thermal conductivity detector. The mixed gas flow was 60 ml min^{-1}. 50 mg of each sample was reduced within the 300 to 1273 K temperature range, using a heating rate of 10 K min^{-1}.

The transmission electron microscopy (TEM) analyses were performed in a JEOL 100-CX-II Microscope. The samples were placed in a graphite cell with HF pretreatment at room temperature. The scanning of samples was adjusted to observe in focus. TEM observations were made under a 100 kV accelerating voltage and a magnification of the order of 400 K×.

The pyridine thermal desorption experiments were accomplished in an infrared spectrometer Nicolet 170 SX. The samples were mounted in a glass cell with a KBr window, which permitted to follow the spectral changes with thermal treatments. The pyridine thermoprogrammed desorption was performed at room temperature and at 323, 373, 473, 573 and 673 K, recording the FTIR signal at each desorption temperature.

The X-ray diffraction patterns of the samples were obtained with a SIEMENS 5000 series, with CuKα radiation without filter, at a 35 kV and 25 mA. The XRD broadening/sharpening of the signal was taken as a comparative measurement of the dispersion of the supported catalysts and correspond to the γ-Al_2O_3 (400) and (440) structural planes. The 2θ angle range was of 20° to 100°.

2.2.1. Activity tests

Catalysts activity tests were carried out in gas oil hydrotreating: hydrogenation of aromatics (HDA), hydrodesulfurization (HDS) and hydrodenitrogenation (HDN) reactions. The evaluations were performed in a continuous down flow high-pressure fixed bed unit using Heavy gas oil (HGO) as a real feedstock, supplied by a Mexican refinery. The reaction conditions used for the catalytic tests were: 54 kg cm^{-2} total pressure, 613–653 K reaction temperature, 2 h^{-1} liquid hourly space velocity (LHSV), H_2/HC ratio = 0.45 m^3 l^{-1} L/L (SCTP), and 5 cm^3 catalyst volume. Prior to catalytic evaluation, the NiMo oxides catalysts were sulfided *in situ*, with a naphtha spiked with CS_2 to reach a 4600 wt. ppm sulfur content at 623 K for 12 h. Operating conditions and feed characterization are summarized in Table 1. Total sulfur, total nitrogen and aromatics content in the feedstock were determined by the D-4292, D-4629 and D-5186 ASTM methods, respectively.

The reactor temperature for the activation was 613 K. In order to maintain constant the reaction conditions, a 12-h stabilization period was imposed. The gaseous reaction products were analyzed by gas chromatography using an HP-5890 GC with a thermal conductivity detector.

The catalytic activity was calculated with a pseudo first order reaction with respect to the organic reactant

Table 1
Operating conditions and feed properties used during catalytic tests

Feed composition	
S_T (wt. ppm)	13985
N_T (wt. ppm)	470
Mono aromatics (wt.%)	15.1
Di-aromatics (wt.%)	12.1
Poly-aromatics (wt.%)	6
Total aromatics (wt.%)	33.2
Activation (CS_2)	
H_2 flow (l h^{-1})	13.4
Liquid flow (ml h^{-1})	30
Pressure (kg cm^{-2})	54
Temperature (K)	503
Stabilization (h)	4
Hydrodesulfurization	
Density (g ml^{-1})	0.8581
Liquid flow (ml h^{-1})	20
H_2 flow (l h^{-1})	8.9
Pressure (kg cm^{-2})	54
Temperature (K)	613, 633, 653
LHSV (h^{-1})	2
H_2/HC (m^3 l^{-1})	0.45

containing nitrogen and aromatics, whereas for the HDS the rate constant was taken to be on the order of 1.5 [13].

$$k_{HDN} = \ln\left(\frac{N_f}{N_p}\right)\mathrm{LHSV} \quad (1)$$

$$k_{HDA} = \ln\left(\frac{A_f}{A_p}\right)\mathrm{LHSV} \quad (2)$$

$$k_{HDS} = \left(\frac{1}{S_p^{0.5}} - \frac{1}{S_f^{0.5}}\right).2\mathrm{LHSV} \quad (3)$$

where k is the apparent constant rate for the removal of nitrogen, total aromatics and sulfur, respectively. A_p, N_p, S_p, are nitrogen, total aromatics and sulfur contents in gas oil hydrotreated (wt. ppm). N_f, A_f, S_f are nitrogen, total aromatics and sulfur contents in feed heavy gas oil (wt.%) and LHSV is the liquid hourly space velocity (h^{-1}).

3. Results and discussion

3.1. Characterization and textural properties

This study presents the influence of metallic particle size on the catalytic activities for the HDS, HDN and HDA reactions of three different NiMo catalysts supported on three different γ-Al_2O_3 supports.

Pore distribution profiles of the studied supports and catalysts are shown in Fig. 1a–b. It can be observed that surface area of support A is the highest (261 m^2 g^{-1}) and the lowest is for C support (176 m^2 g^{-1}). Surface areas for the supports decreases in the following order C<B<A (Fig. 1a). The mean pore distribution of the supports is monomodal in all the cases. A support exhibited a mean pore distribution around 70, and has a maximum pore volume of 1.4 cm^3 g^{-1}. Supports with 5 and 10 nm (B and C) displayed an average pore diameter around 95 and 93, respectively, having a pore volume greater than 2.0 cm^3 g^{-1}.

As can be observed in Fig. 1b the surface areas of fresh catalysts decrease because the metal loading. Catalysts NiMo-A decreases about 23%, while in catalysts NiMo-B and C this reduction was around 14% and 13%, respectively (Table 2).

Pore volumes and median pore distribution of fresh catalysts also decrease compared with the support ones.

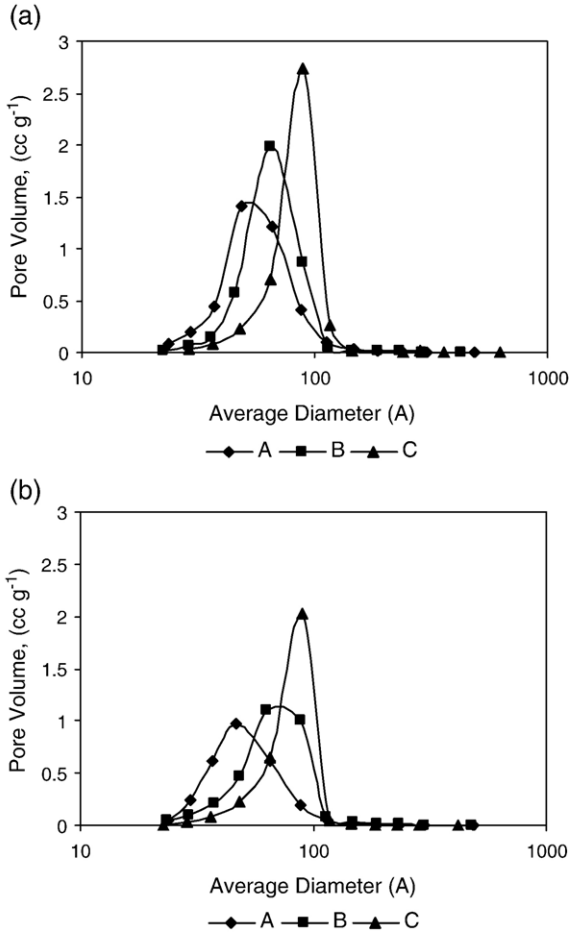

Fig. 1. Pore distribution profiles of the studied samples: (a) supports and (b) catalysts.

Table 2
Textural properties of NiMo/γ-Al_2O_3 catalysts using different supports

Catalyst	Surface area ($m^2\ g^{-1}$)	Average diameter (Å)	Pore volume ($ml\ g^{-1}$)
NiMo-A	206	64.77	0.33
NiMo-B	183	79.35	0.38
NiMo-C	153	100.38	0.38

It can be seen that this diminishing was more important for NiMo-C>NiMo-B>NiMo-A, which suggested that the control of particle size in the alumina support is quite important to obtain a suitable ratio (surface area/pore volume) and get active sites.

3.2. TPD

Fig. 2 shows the total acidity measured by pyridine TPD, where A has the higher acidity than B and C samples. The three supports showed medium strength sites that were desorbed until 573 K. The Lewis acidity on the supports and the force of acid sites is in the following order A>B>C. This means that A support could stabilize the metastable dispersion of small metallic particles on the alumina surface avoiding agglomeration and sintering.

Some studies have suggested correlations between the activity and acidity characteristics of the catalyst in the oxidic state, which also depends of the support's textural properties [14]. In the case of sulfided unpromoted catalysts, Cowley and Massoth [15] found that HDS activity decreased linearly with amount of pyridine present on the surface catalysts. Furthermore, these authors found that the amount of pyridine adsorbed correspond to the concentration of anion vacancies which may regarded as Lewis acid sites. These results imply that one could expect to observe good correlations between activity and the amount of pyridine adsorbed for promoted catalyst and dispersed the metallic particles as our TPD measurements suggested.

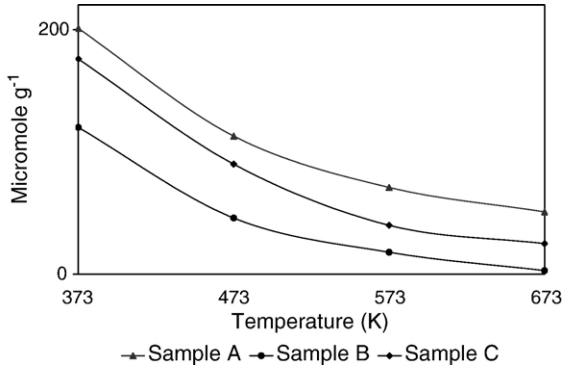

Fig. 2. Total acidity of alumina supports with different crystal size (3, 5 and 10 nm).

3.3. XRD

The XRD patterns of the synthesized supports are shown in Fig. 3a. A decrease in the intensity of the γ-Al_2O_3 (311), (400), (440) planes was observed when the crystal size was smaller (according to JCPDS 10-425). The broadening of these peaks was higher also with smaller alumina particle size. As a preliminary approximation, the average particle size for each support before their impregnation was calculated using Scherrer's equation.

$$D_{hkl} = \frac{0.9\lambda}{\beta \cos\theta} \tag{4}$$

where D_{hkl} is the average crystal size, λ the X-ray wavelength, β the FWHM of the (hkl) reflection peak and θ is the Bragg angle.

The particle sizes calculated for each γ-Al_2O_3 support at the characteristic crystalline planes were: 400 (3.5, 4.7 and 9.6 nm), and 440 (3.8, 4.8 and 9.8 nm),

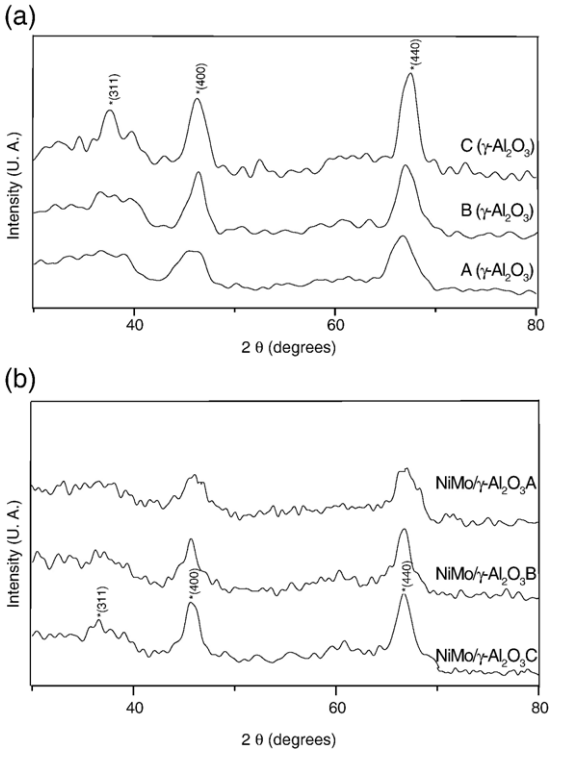

Fig. 3. XRD patterns for (a) γ-Al_2O_3 support and (b) NiMo catalyst oxides after calcinations at 773 K.

respectively. Fig. 3b also shows the XRD pattern for the NiMo/γ-Al_2O_3 catalysts annealed at 773 K. A deformed peak can be observed for the A support at $2\theta = 45.862°$ and $2\theta = 67.032°$, which indicates that the crystal size has changed when the NiMo catalyst was sintered. In accordance with the preparation of NiMo/γ-Al_2O_3 catalyst, the predominant Mo oxide species is highly dispersed on substrate surface and they can not be identified by diffraction patterns [16,17].

3.4. TPR studies

TPR profiles of A, B and C NiMo oxide catalysts annealed at 773 K containing equal molybdenum and nickel loadings (11.5 wt.% and 2.9 wt.%) are presented in Fig. 4.

These results were carried out in the temperature range of 300 to 1273 K showing two characteristic peaks for NiMo catalysts at 750 K and 1100 K which have been previously reported [18–21]. All samples showed similar features with some changes in the intensity. In each case the T_m value (defined for the temperature of maximum H_2 consumption, i.e. the peak maximum) is displayed alongside the corresponding TPR signal.

The first peak (lower $T_m = 750$ K) has been attributed to the reduction of Mo^{6+} to Mo^{4+} of polymeric Mo structures; this strong reduction is carried out due to the strong interaction between molybdenum and alumina and because the less-polarized bonds of poly-molybdates are more easily reducible that those species directly bonded to alumina [18–21]. Spojakina et al. [22] concluded that Mo^{6+} species in molybdenum catalysts depend on the composition of the support surface, however our TPR studies with the same Mo loading and the differences in the hydrogen consumption are correlated to the crystal size of the alumina support (Table 3).

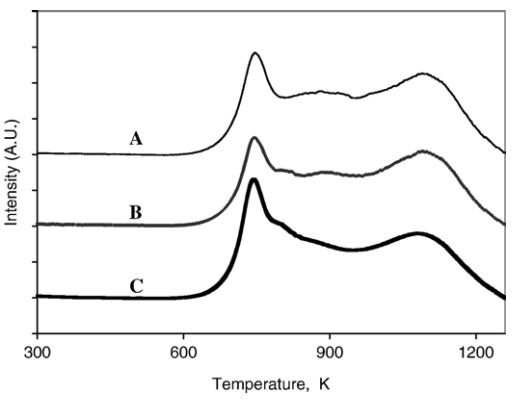

Fig. 4. H_2 TPR profiles of A, B, and C NiMo/γ-Al_2O_3 catalysts calcined at 773 K using different crystal sizes in the supports.

Table 3
H_2 TPR deconvolution and H_2 consumption for obtained profiles (A.U.)

Catalyst	1st peak (745 K)	2nd peak (880 K)	3rd peak (800 K)	4th peak (1100 K)	Total consumption, H_2 (A.U.)
A	5930	23405	1514 (1001)	17063	47911
B	5132	21997	698	15031	42859
C	6625	19608	1509	16538	44280

Therefore, TPR studies revealed that the predominant poly-molybdates species with octahedral-coordinated Mo^{6+} interact strongly in the alumina support and the effect of the polarization of alumina affect directly the covalence of Mo–O bonds, thus causing a reducer atmosphere [22]. The last peak is generally associated with a further progress in the reduction of Mo species of the first peak, together with the partial reduction of strongly Al_2O_3 interacting with coordinated tetrahedral Mo species (Mo^{3+} to Mo^{2+}).

These results show that Ni originates a light shoulder in the intermediate temperature region between 823 and 1050 K, which overlaps with the high temperature peak; as we know, this feature of TPR complicates their interpretation because of the Ni species that are involved at the reduction regions. Although exist two possible Ni^{2+} species, in the region between 823 and 1050 K, respectively, only we can identify one of them, which is attributed to the reduction of a dispersed NiO phase weakly bound to γ-Al_2O_3 surface. Table 3 summarizes the quantitative TPR data and temperature of the maximums encountered by deconvolution and profile integration, for the total H_2 consumption and reduction degrees values. No clear trend was observed for the catalysts with different crystal size, except higher H_2 consumption at dispersed NiO (catalyst A) compared to the first and third peaks in the same sample.

Because of the higher hydrogen consumption at 1100 K (T_m), the samples showed strong interactions with the tetrahedral sites of the molybdenum supported on alumina avoiding a higher reduction degree. Brito et al. [18,19,21] found that bulk NiO reduced before 573 K, but when it is supported on alumina, the peak appears at 973 K. Hence, in our TPR profiles, the shoulder peak between 823 and 1050 K could be attributed to the formation of $NiMoO_4$ phase [22], wherein the role of Ni as a reduction promoter of the molybdenum could be confirmed. This effect is favored with the increased acidity of the alumina support and the decreased crystal size (see Figs. 2 and 3). However, the study of NiMo/Al_2O_3 catalysts by Burch and Collins [23] suggested that most of the nickel reduces simultaneously with the molybdenum at similar temperature (773 K), but a

substantial part of the nickel reduces until 850 K in the NiMo catalyst samples. Then in this work, it seems to be that Ni does not modify the nature of the MoO_3 multilayer, but it is favoring its reduction.

3.5. TEM micrographs

TEM micrographs of NiMo oxides supported on alumina for each sample show the particle size and metallic dispersion after the NiMo spray impregnation and annealing processes (see Fig. 5). The samples were studied after hydrofluoric treatment [24]. These TEM images were obtained by replica and magnified ×400 000.

The TEM micrographs show heterogeneity of metallic particle sizes for the three NiMo catalysts (A, B and C) which can be considered an effect of the textural properties.

These results showed that NiMo-A catalyst presents higher uniformity of the metallic particles than those for B and C. The crystalline region for each one and its distribution can be seen in these micrographs (Fig. 5), which also show that the metallic particles had irregular shapes. The comparison of the three materials demonstrated that A support allows to obtain the smallest metallic particle size distribution measured as well as a higher dispersion.

The metallic particle size distribution for the NiMo oxide catalyst annealed at 773 K were about 2 and 4 nm. A catalyst showed a around 91.9% and 8.1% for 2 nm and 4 nm, respectively, while B catalyst was between 74.6% and 23.3% and C catalyst was between 92.3% and 7.7%, for 2 and 4 nm, respectively. The mean particle size was 2.16, 2.43 and 2.25 nm for A, B, and C oxides NiMo on the alumina surface.

According to the results obtained on the metallic particles size observed by TEM, it can be presumed that the Ni–Mo species are well dispersed over the support and is possibly located at the edges of MoO^3 particles [5].

The discrepancies found in the particle size obtained for the annealed catalysts could be explained by the following factors; firstly, it appears necessary to recall that care must be taken for the adsorption and diffusion effects during catalyst preparation that can influence growth MoO_3 species. These phenomena seem to agree with the average pore diameter and pore volume found during textural measurements. Another important

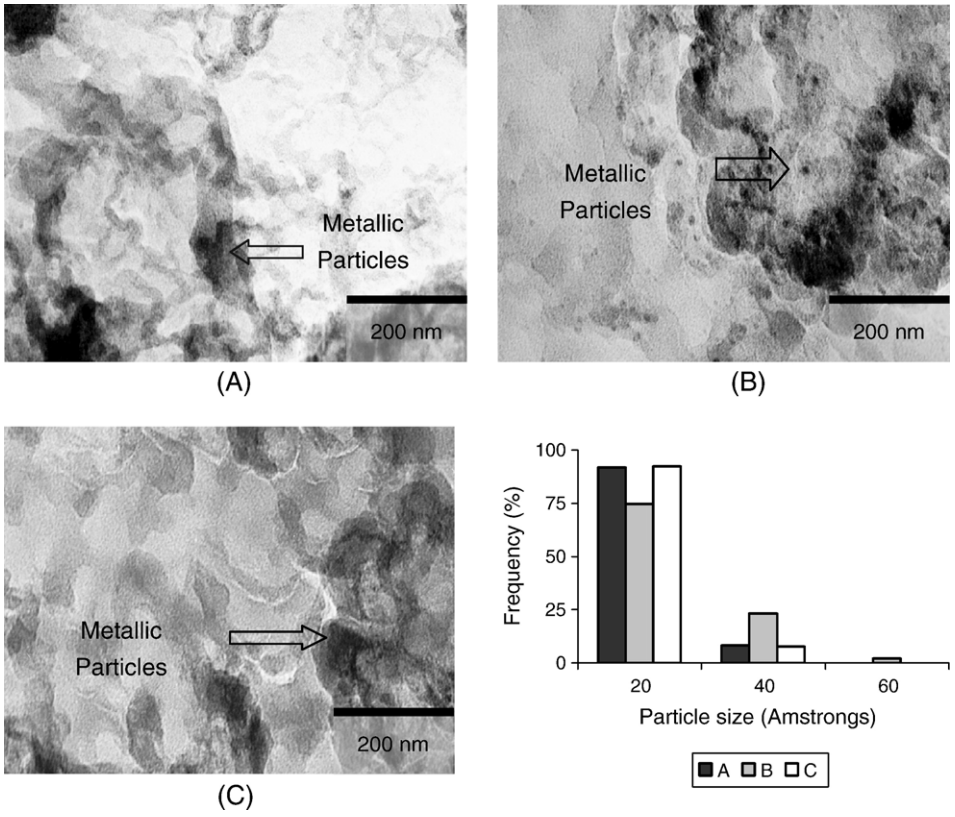

Fig. 5. TEM micrographs and crystal size distribution of NiMo oxides catalysts supported on A (3 nm), B (5 nm) and C (10 nm) supports. ×400 000 and 100 kV.

factors are the formation of oxidic species which could depend on the hydration state of the oxidic precursor, the temperature and duration of the annealed, but in this case these variables were maintained constant during catalysts preparation.

TEM micrographs for the metallic particle size of sulfided NiMo catalysts show a decrease of crystal size compared with the oxide NiMo catalysts. The particles obtained over the sulfided samples were predominantly 2 nm (see Fig. 6). The mean particle size was 2.03, 2.08 and 2.23 nm for A, B and C NiMo sulfides on the alumina surface.

It can be seen that the reduction in particle size for the different NiMoS species is more influenced by the textural properties than by oxidic species. This may be attributed to the oxygen substitution by sulfur to obtain nickel sulfide and MoS_2 species, which would exert a decrease in the final particle size, as it was observed. Another reason could be that single layers of MoS_2 dominate the structure (S–Mo–S) and these can be oriented with the basal planes approximately perpendicular to the support surface after sulfidation, which can be seriously affected by the morphology and affecting the formation of small MoS_2 particles [10]. In addition, some researches mentioned that more than 90% of Mo species are transformed during sulphidation into MoS_2 supported state with a layer structure. This layer forms weak van der Waals interactions between two successive layers (Mo–Mo) giving some interesting properties to MoS_2 such as; within the MoS_2 layer MoIV is bound to six sulphur ions (S^{2-}) in a trigonal prismatic coordination, which can cause an inhibition in their growth [25].

Then, as a consequence of the particle size for each support, it was assumed that the sulfided NiMo catalysts have an uniform bond for each support. For example, the A catalyst has a higher dispersion than the others, which may be due to the surface orientation of γ-Al_2O_3 that plays an important role on the MoS_2 microstructures [10]. In the present case, it was attempted to evaluate the positive effect of small particle size alumina: A, B and C. In fact, the lateral size of the MoS_2 structures is an important parameter during preparation of the hydrotreating catalyst; however, they are too small to be observed by TEM.

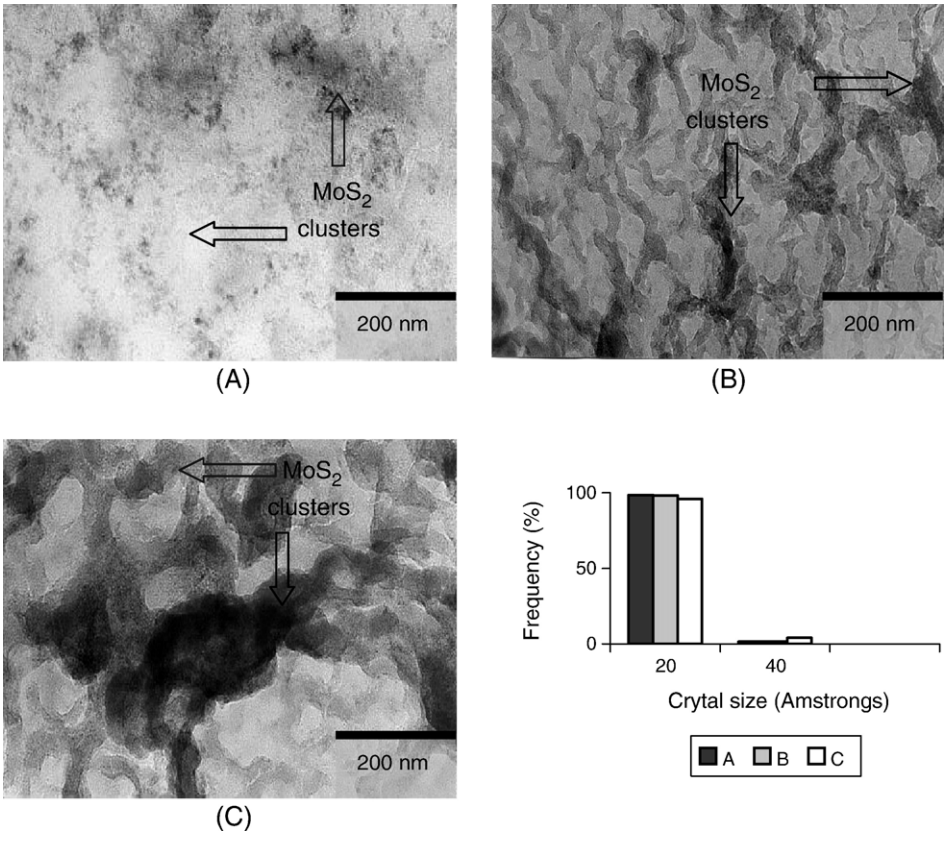

Fig. 6. TEM micrographs and crystal size distribution of NiMoS catalysts supported on A (3 nm), B (5 nm) and C (10 nm) supports. ×400 000 and 100 kV.

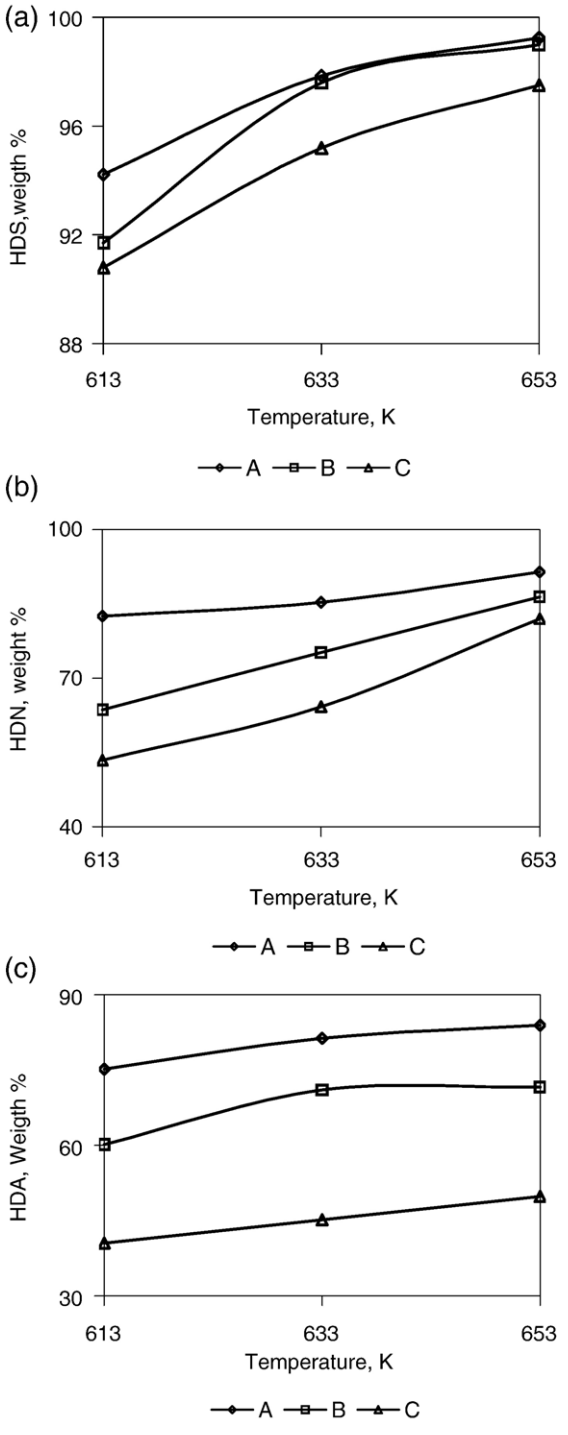

Fig. 7. Effect of reaction temperature on (a) HDS, (b) HDN and (c) HDA activity, according to the crystal size of γ-Al_2O_3 supports used.

If we assume that the alumina particle sizes are no greater than 10 nm in all the specimens, it is quite reasonable to assume that the MoS_2 are "step-kinked" or bent to conform the alumina surface, and may that this cannot be observed in the micrographs, although it is required to consider some structural arrangements at the

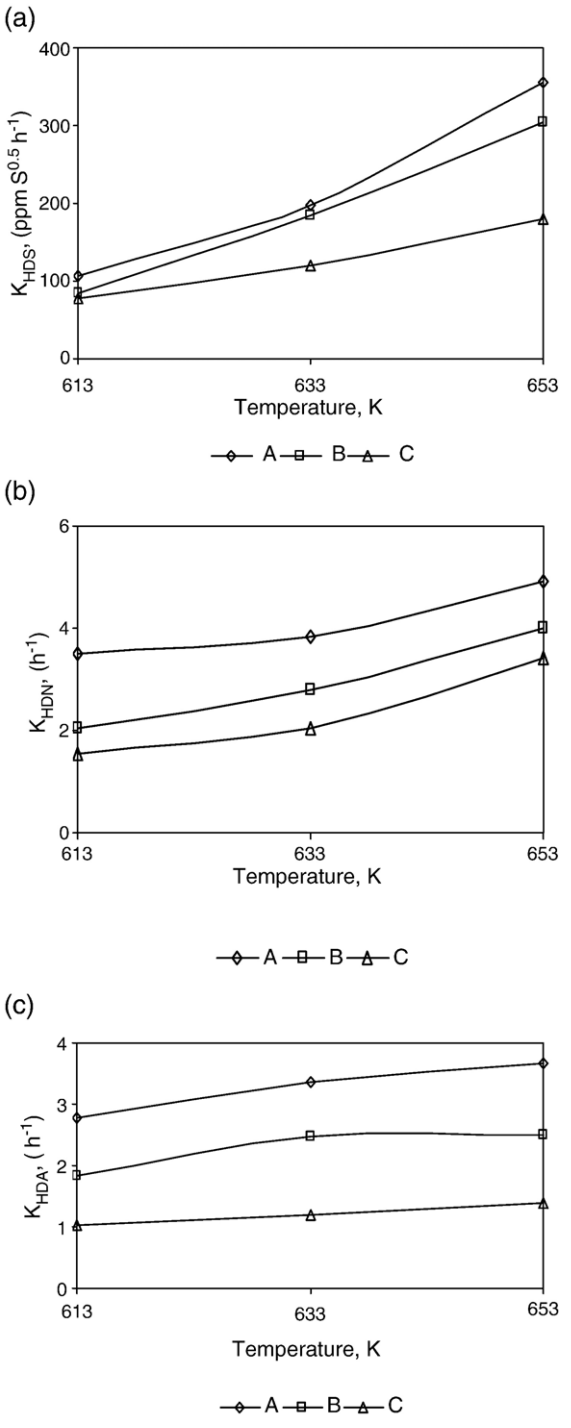

Fig. 8. Apparent constant rates for the NiMoS/γ-Al_2O_3 (A=3, B=5 and C=10 nm) catalysts at P=54 kg cm^{-2} and T=613–553 K: (a) HDS; (b) HDN and (c) HDA.

edges and corners of the small MoS_2 crystals that could be displaced from their ideal MoS_2 lattice toward positions of higher stability as some researches have showed [10,11].

3.6. HDS, HDN and HDA activities

The effect of the metallic particle size of the NiMo-A, -B or -C/γ-Al_2O_3 catalysts was correlated with their hydrotreating catalytic activity (HDS, HDN and HDA) in the 613–653 K reaction temperature range and 54 kg cm^{-2} pressure (see Figs. 7 and 8).

Under the experimental conditions, the catalysts deactivate slowly with smaller particles size of the support. It can be seen as a consequence that Ni–Mo/γ-Al_2O_3–A was more active than NiMo/γ-Al_2O_3 (B and C) particularly for the HDS reaction, although the same effect can be observed in the HDN and HDA reactions. In general, these curves also displayed that all the samples increased their catalytic activity with the temperature.

The nitrogen removal for each support was also increased with smaller NiMoS particles size. The elimination of nitrogen compounds was about 86 wt.% less than HDS, because nitrogen removal requires more severity in the operating conditions. At 653 K reactor temperature, a maximum contaminants quantity was removed; the specific conversion for HDS, HDN and HDA for NiMo/γ-Al_2O_3–A catalyst (99.25%, and 91.48% and 83.95%, respectively).

Fig. 8 relates the effect of the apparent constant rates k_{HDS}, k_{HDN} and k_{HDN} for hydrotreating reactions. The increase of the k_{HDS}, k_{HDN}, and k_{HDA} at the different temperatures indicates that temperature, and the type of alumina support favors these reactions. It is clear that for the NiMo-A, -B, -C/γ-Al_2O_3 catalysts, the catalytic activity reached a maximum at 653 K but, at the same temperature, this catalytic activity for B and C supports is less important than that for A.

The importance ascribed to the differences between the alumina support, the active phases and the catalytic behavior, improves the catalysts design importance in order to obtain better hydrotreating catalysts.

The higher HDS, HDN and HDA intrinsic activity of NiMo/γ-Al_2O_3–A catalyst compared with the other ones may be attributed to the more homogeneous distribution of MoS_2 and nickel sulfide and its location on alumina surface and, although this activity differs considerably from MoS_2 particle size measurements, it is necessary to consider other factors such as synergistic effect during MoS_2 and nickel sulfide formation, which could be located in close vicinity of acid sites and diffusional effects [26–28].

4. Conclusions

Three types of alumina supports were studied in the HDS, HDN and HDA reactions having three different particle sizes. The correlation of particle size of the alumina support, NiMo oxide catalysts, and finally NiMoS catalyst, was important to determine the changes of the active sites after the annealing and sulfidation steps. The experimental data relative to the catalytic activity for HDS, HDN and HDA showed that they depend on the alumina particle size and on the NiMo species metallic particle size. Significant reduction (99.25 wt.%) in the sulfur content of the treated heavy gas oil could be achieved over NiMo-A catalyst at 653 K using a support with crystal size of about 3 nm. From the comparison of the XRD results and TEM micrographs, it became evident how the distribution of the surface NiMo species could influence the catalytic activity of the HDS, HDN and HDA reactions. A maximum for the HDS, HDN and HDA reaction rates was observed at 653 K for catalyst-A where the particle size of the support was smaller. The change of interaction between NiMoS and γ-Al_2O_3 measured as the effect of particle size of the support and catalytic activity is proportional to the reactor temperature studied.

Acknowledgments

Authors thank the financial support from Instituto Mexicano del Petroleo (D.01017), CGPI-IPN and CONACYT.

References

[1] Knudsen KG, Cooper BH, Topsøe H. Catalyst and process technologies for ultra low sulfur diesel. Appl Catal A Gen 1999;189:205.
[2] Babich IV, Moulijn JA. Science and technology of novel processes for deep desulfurization of oil refinery streams: a review. Fuel 2003;82:607.
[3] Scheffer B, Mangnus PJ, Moulijn JA. J Catal 1990;121:18.
[4] Weisser O, Landa S. Sulfide catalysts; their properties and applications. New York, NY: Pergamon-Press; 1973.
[5] Topsøe H, Clausen BS, Massoth FE. Hydrotreating catalysts. Berlin, Heidelberg: Springer-Verlag; 1996.
[6] Lecrenay E, Sakanishi K, Nagamatsu T, Mochida I, Suzuka T. Hydrodesulfurization activity of CoMo and NiMo supported on Al_2O_3–TiO_2 for some model compounds and gas oils. Appl Catal B Environ 1998;18:325.
[7] Prings R, de Beer VHJ, Somorjai GA. Structure and function of the catalysts and the promoter in Co–Mo hydrodesulfurization catalysts. Catal Rev Sci Eng 1989;31:1.
[8] Lauritsen JV, Helveg S, Laegsgaard E, Clausen BS, Topsøe H, Besenbacher F. Atomic-scale structure of Co–MoS nanoclusters in hydrotreating catalysts. J Catal 2001;97:1.

[9] Shimada H, Sato T, Yoshimura Y, Hiraishi J, Nishijima A. Support effect on the catalytic activity and properties of sulfided molybdenum catalysts. J Catal 1988;110:275.
[10] Sakashita Y, Yoneda T. Orientation of MoS_2 clusters supported on two kinds of γ-Al_2O_3 single crystal surfaces with different indices. J Catal 1999;185:487.
[11] Sakashita Y, Araki Y, Shimadam H. Effect of surface orientation of alumina supports on the catalytic functionality of molybdenum sulfide catalysts. Appl Catal A Gen 2001;215:101.
[12] Laine J, Brito JL, Severino F. Carbon deposition and hydrodesulfurization of Nickel–Molybdenum supported catalysts. Appl Catal A Gen 1985;15:333.
[13] Bej SK, Dalai AK, Adjaye F. Kinetics of hydrodesulfurization of heavy gas oil derived from oil–sands bitumen. Pet Sci Technol 2002;20:867.
[14] Laine J, Brito J, Yunes S. In: Barry HF, Mitchell PCH, editors. Proc 3rd Int. conf. on chemistry and uses of molybdenum, Climax Molybdenum Company; 1979. p. 111.
[15] Cowley SW, Massoth FE. J Catal 1978;51:279.
[16] Hall WK, Vanselow R, Howe R, editors. Chemistry and physics solid surfaces, vol. 4. Berlin, Heidelberg: Springer-Verlag; 1986. p. 73.
[17] Okamoto Y, Imanaka T. Interaction chemistry between molybdena and alumina: infrared studies of surface hydroxyl groups and adsorbed carbon dioxide on alumina modified with molybdate, sulfate, or fluoride anions. J Phys Chem 1988;92:7102.
[18] Brito JL, Laine J. Reducibility of Ni–Mo/Al_2O_3 catalysts: a TPR study. J Catal 1993;139:540.
[19] Brito JL, Laine J. Temperature-programmed reduction of Ni–Mo oxides. Mater Sci 1989;24:425.
[20] López-Cordero R, López-Agudo A. Effect of water extraction on the surface properties of Mo/Al_2O_3 hytrotreating catalysts. Appl Catal A Gen 2000;202:23.
[21] Brito JL, Laine J. Characterization of supported MoO_3 by temperature-programmed reduction. J Catal 1986;5:179.
[22] Spojakina A, Damyyanova S, Jiratova K. In: Nogueira L, Zam YL, editors. Brasil, proceedings of XII simposio iberoamericano de catálisis; 1990. p. 571.
[23] Burch R, Collins A. Temperature-programmed reduction of Ni/Mo hydrotreating catalysts. Appl Catal A Gen 1995;18:389.
[24] Eijsbouts S. In: Delmon B, Froment GF, Grange P, editors. Life cycle of hydroprocessing catalysts and total catalyst management, vol. 21. Elsevier Science; 1999.
[25] Grimblot J. Genesis, architecture and nature of sites of Co(Ni)–MoS_2 supported hydroprocessing catalysts. Catal Today 1998;41:111.
[26] Dufresne P, Payen E, Grimblot J, Bonnelle JP. Study of Ni–Mo–γ-Al_2O_3 catalysts by X-ray photoelectron and Raman spectroscopy comparison with Co–Mo–γ-Al_2O_3 catalysts. Phys Chem 1981;85:2344.
[27] Damyanova S, Spojakina A, Jiratova K. Effect of mixed titania–alumina supports on the phase composition of NiMo/TiO_2–Al_2O_3 catalysts. Appl Catal A Gen 1995;125:257.
[28] Cáceres C, Fierro JLG, López-Agudo A, Severino F, Laine J. Relation between hydrodesulfurization activity and the state of promoters in precursor calcined Ni–Co–Mo/Al_2O_3 catalysts. J Catal 1986;97:219.